Supporting information

for

Silver Complex with an *N*,*S*,*S*-Macrocyclic Ligand Bearing an Anthracene Pendant Arm for Optical Ethylene Monitoring

Yutaka Hitomi,* Toshiyuki Nagai and Masahito Kodera

Department of Molecular Chemistry and Biochemistry, Doshisha University

1-3 Tatara Miyakodani, Kyototanabe, Kyoto 610-0321, Japan

Contents

Experimental section

Experimental Procedure

General. All chemicals used in this study were commercial products of the highest available purity and were further purified by the standard methods, if necessary.[S1] Anhydrous MeCN for organic synthesis and optical-grade solvents for analysis were purchased from Wako Pure Chemicals Industries, Ltd. (Osaka, Japan). 8-Aza-1,5-dithiacyclodecane was prepared according to the literature.[S2] FT-IR spectra were recorded on a Shimadzu IRAffinity-1 FTIR spectrometer equipped with a MIRacle10 single reflection ATR accessory. UV-visible spectra were taken on an Agilent 8543 UV-visible spectrophotometer equipped with a thermostated cell compartment controlled by a NESLAB circulation system. Fluorescence spectra were measured on a Hitachi F-7000 spectrophotometer. ^{1}H- and ^{13}C-NMR spectra were recorded on a JEOL JMN-A 500 spectrometer. Electrospray ionisation mass spectra measurements were performed on a JEOL JMS-T100CS spectrometer. Elemental analyses were carried out with a Perkin-Elmer Elemental Analyzer 2400 II.

Synthesis of *N*-[(9-anthracenyl)methyl]-1-aza-4,8-dithiacyclodecane (L1)

To a solution of 8-aza-1,5-dithiacyclodecane (250 mg, 0.98 mmol) and K_2CO_3 (1.0 g, 7.25 mmol) in dry MeCN (6 mL) was added a solution of 9-chloromethylanthracene (200 mg, 1.12 mmol) in MeCN (4 mL) under N_2. The mixture was stirred at room temperature. The progress of the reaction was followed by TLC (alumina, R_f = 0.2, CH_2Cl_2/hexane = 2:5). After stirring 4 days, the mixture was filtered through a Celite® 545 pad. The filtrate was concentrated and purified by alumina column chromatography (CH_2Cl_2/hexane = 2:5) to afford **L1** as white solid (160 mg, 48%). ^{1}H NMR (500 MHz, in acetone-d_6): δ1.73-1.68 (m, -S-CH_2-CH_2-CH_2-S, 2H), 2.45-2.43 (m, -S-CH_2-CH_2-N, 4H), 3.05-3.01 (m, CH_2-S-CH_2-CH_2-N, 8H), 4.63 (s, An-CH_2-N, 2H), 7.51 (dd, *J* = 8.1, 6.7 Hz, An3 or An 6, 2H), 7.57 (dd, *J* = 8.9, 6.7 Hz, An2 or An7, 2H), 8.09 (d, *J* = 8.1 Hz, An4 or An5, 1H), 8.57 (s, An10, 1H), 8.82 (d, *J* = 8.9 Hz, An1 or An8, 2H). ^{13}C NMR (125.8 MHz, $CDCl_3$): δ 30.6 (-S-CH_2-*C*H_2-CH_2-S), 30.6 (*C*H_2-S-CH_2-CH_2-N), 33.3 (-S-*C*H_2-CH_2-N), 53.03 (An-*C*H_2-N), 58.4 (S-CH_2-*C*H_2-N), 126.5 (An3/An6), 126.8 (An2/An7), 128.5 (An1/An8), 129.1 (An10), 129.8 (An4/An5), 131.2 (An9), 132.3 (An4a/An10a), 132.5 (An8a/An9a). Anal. Calcd for $C_{23}H_{25}NS_2$: C, 71.89; H, 6.86; N, 3.81. Found: C, 71.80; H, 7.18; N, 3.65. ESI-MS (*m*/*z*): $[M + H]^+$ calcd for $C_{22}H_{28}NS_2$, 368.15; found, 368.19.

Synthesis of [Ag(L1)]OTf (1).

To a solution of **L1** (30 mg, 0.82 mmol) in dry THF (2 mL) was added a solution of AgOTf (21 mg, 0.82 mmol) in dry THF (1 mL). After stirring for 1 h at room temperature, hexane (2 mL) was added to the mixture to give a yellowish white solid. The solid was washed with hexane and then dried thoroughly *in vacuo* to obtain [Ag(**L1**)]OTf. Yield 40 mg (78%). ^{1}H NMR (500 MHz, in acetone-d_6): δ 3.11-1.35 (br, S-CH_2-CH_2-CH_2-S-CH_2-CH_2-N, 14H), 5.05 (s, An-CH_2-N, 2H), 7.60(dd, *J* = 8.6, 6.2 Hz, 2H), 7.74 (dd, *J* = 9.1, 6.2 Hz, 2H), 8.21 (d, *J* = 8.6 Hz, 1H), 8.71 (s, 1H), 8.73 (d, *J* = 9.1 Hz, 2H). ^{13}C NMR (125.8 MHz, $CDCl_3$): 31.7 (-S-CH_2-*C*H_2-CH_2-S), 33.2 (*C*H_2-S-CH_2-CH_2-N), 35.0 (-S-*C*H_2-CH_2-N), 52.0 (S-CH_2-*C*H_2-N), 52.4 (An-*C*H_2-N),

120.3 (An1/An8), 126.4 (An3/An6), 128.4 (An2/An7), 129.9 (An10), 130.4 (An9), 131.4 (An4/An5), 132.0 (An8a/An9a), 132.5 (An4a/10a). Anal. Calcd for $C_{23}H_{25}AgF_3NO_3S_2$: C, 44.23; H, 4.03; N, 2.24. Found: C, 44.11; H, 4.20; N, 2.10. UV-vis ($CHCl_3$): 358 nm (4381 dm^3 mol^{-1} cm^{-1}), 375 nm (6487 dm^3 mol^{-1} cm^{-1}), 395 nm (5709 dm^3 mol^{-1} cm^{-1}). ESI-MS (*m*/*z*): $[M]^+$ calcd for $C_{22}H_{27}AgNS_2$, 474.05, 476.05; found, 474.01, 476.01.

Electronic absorption titration study of L1 with AgOTf.

Electronic absorption spectra were measured on an Agilent 8543 UV-visible spectrophotometer at 25°C. Ten portions (5 μL, 0.2 equiv.) of a 2.9 mM solution of AgOTf in MeOH were injected into a solution of **L1** in MeOH (36 μM, 2 mL) in a 1-cm quartz cuvette.

Electronic absorption titration studies of 1 with MeCN and alkenes.

Electronic absorption spectra were measured on an Agilent 8543 UV-visible spectrophotometer at 25°C. Aliquots of MeCN or alkenes were injected into a solution of **1** in chloroform (64 μM, 2 mL) in a 1-cm quartz cuvette.

^{1}H NMR spectroscopic titration study of 1 with MeCN and *cis*-cyclooctene.

^{1}H NMR spectra were measured on a JEOL JMN-A 500 spectrometer at 25°C. Aliquots of MeCN or *cis*-cyclooctene were injected into a solution of **1** in acetone-d_6 (0.5 mM) in a 5-mm NMR sample tube.

Fluorescence titration study of 1 with *cis*-cyclooctene.

Titration study was performed under the same conditions of the above-mentioned electronic absorption titration study. Fluorescence spectra were recorded after each injection with the excitation wavelength at 339 nm and slit widths of 1.0 nm.

Electronic absorption and fluorescence spectroscopy studies on a reversible binding between 1 and ethylene.

The reversible binding studies were performed in a 0.1-cm quartz cuvette equipped with a three-way cock at room temperature. The solution of **1** in chloroform (580 μM) was measured of the electronic absorption and fluorescence spectroscopy in normal transmission and reflection modes, respectively. Fluorescence spectra were recorded with the excitation wavelength at 353 nm, excitation slit width at 1 nm and emission slit width at 10 nm.. Ethylene and nitrogen gasses were repeatedly introduced through a rubber serum cap attached to the three-way cock.

We examined spectral changes of **1** upon purging with ethylene in different solvents; i.e. 2-butanone, methanol, ethyl acetate, tetrahydrofuran, *N*,*N*-dimethylformamide and chloroform, and found that chloroform gave the largest enhancement in the fluorescence intensity. Upon purging with ethylene, the fluorescence intensity of **1** increases ca. 2.0-fold in chloroform, ca. 1.5-fold in *N*,*N*-dimethylformamide, a. 1.4-fold in 2-butanone, ca. 1.3-fold in methanol, ca. 1.3-fold in tetrahydrofuran, and ca. 1.1-fold in ethyl acetate. We did not observe any fluorescence spectral change of **L1** in chloroform upon purging with ethylene.

^{1}H NMR spectroscopic studies on a reversible binding between 1 and ethylene.

The reversible binding study was performed in a 5-mm NMR sample tube equipped with a rubber serum cap on the top at 25°C. Ethylene and nitrogen gasses were repeatedly introduced into a solution of **1** in acetone-d_6 (2.7 mM) through the rubber serum cap. The concentration of ethylene in the solution was estimated based on the peak area of the proton signals of ethylene.

Density functional calculation.

Spin-restricted DFT calculations were performed using the program ORCA version 2.8.[S3] The structure of **1** were fully optimised using the BP method in combination with TZV(2pf) basis sets on Ag, TZV(2d) basis sets on C, N, and S, and TZP(p) basis sets on H.

References

(S1) W. L. F. Armarego, D. D. Perrin, In Purification of Laboratory Chemicals, 4th ed. Butterworth-Heinemann; Oxford, **1996**,176–215.

(S2) S. Chandrasekhar, A. McAuley, *Inorg. Chem.*, **1992,** *31*, 2234–2240.

(S3) F. Neese, ORCA—An ab Initio, Density Functional, and Semiempirical Program Package (Universität Bonn, Bonn, Germany) Version 2.8, 2010.

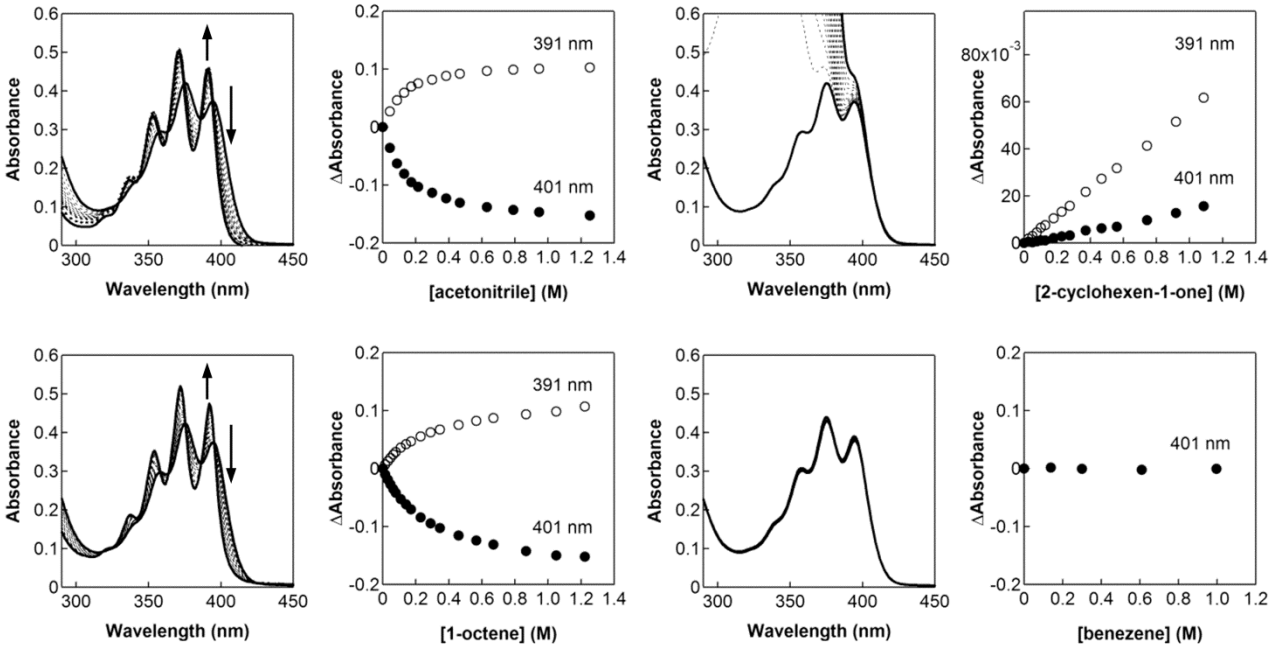

Fig. S1 Electronic absorption spectral changes of **1** (64 μM) in chloroform on titration with acetonitrile (a), 1-octene (b), 2-cyclohexen-1-one (c), and benzene (d). The arrows indicate spectral change with increasing the concentration of alkenes or benzene. The left panels show changes in selected absorbance during the course of the titration. Since 2-cyclohexen-1-one has an absorption band at around 320 nm, we analysed the spectral changes of **1** after subtracting the absorbance derived from 2-cyclohexen-1-one.

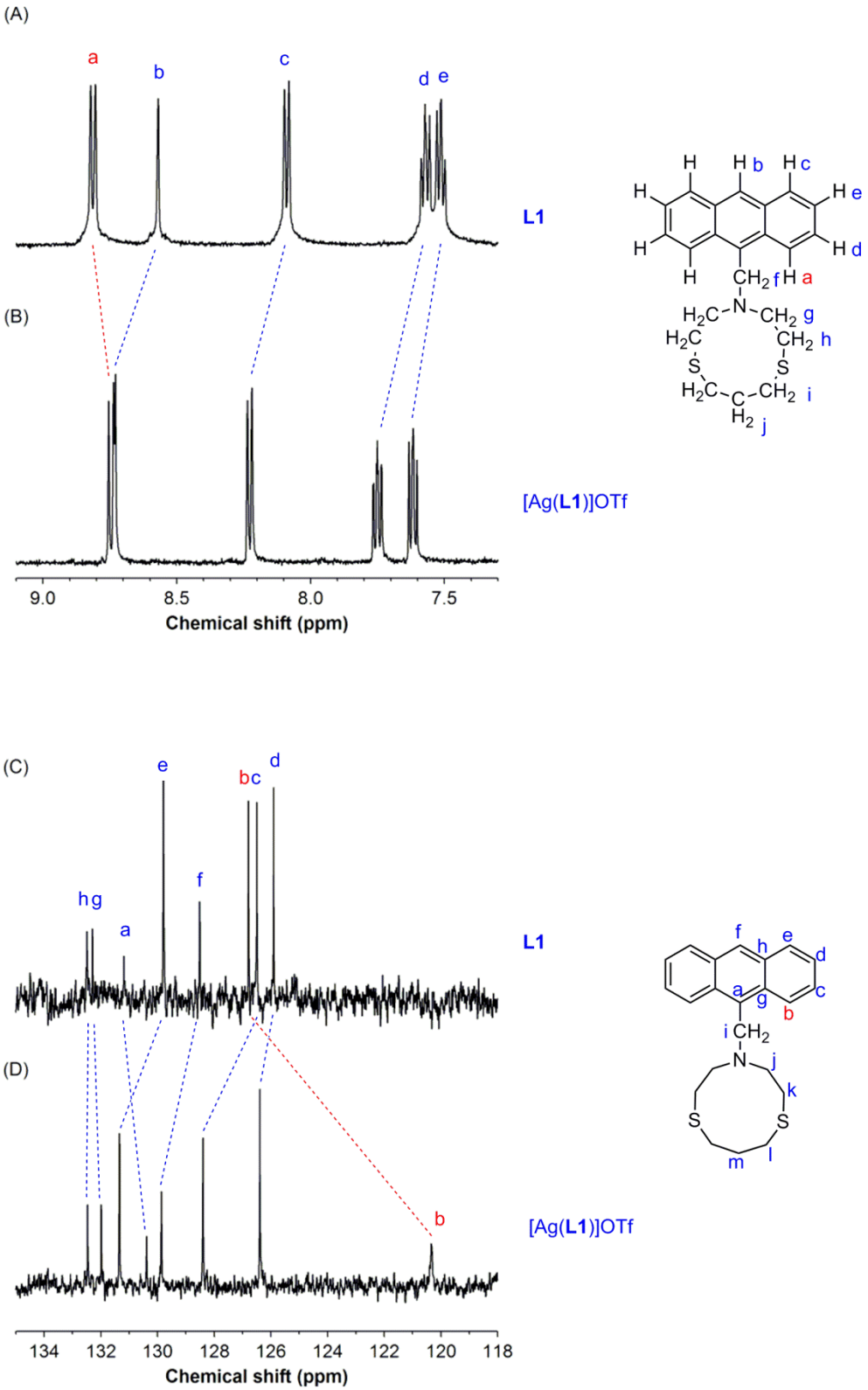

Fig. S2 Aromatic regions in the ^{1}H and ^{13}C NMR spectra of **L1** (A and C) and **1** (B and D) in acetone-d_6. Signals a, b, c, d and e correspond to the protons at 1/8-, 10-, 4/5-, 2/7-, 3/6- positions of the anthracene moiety, respectively.

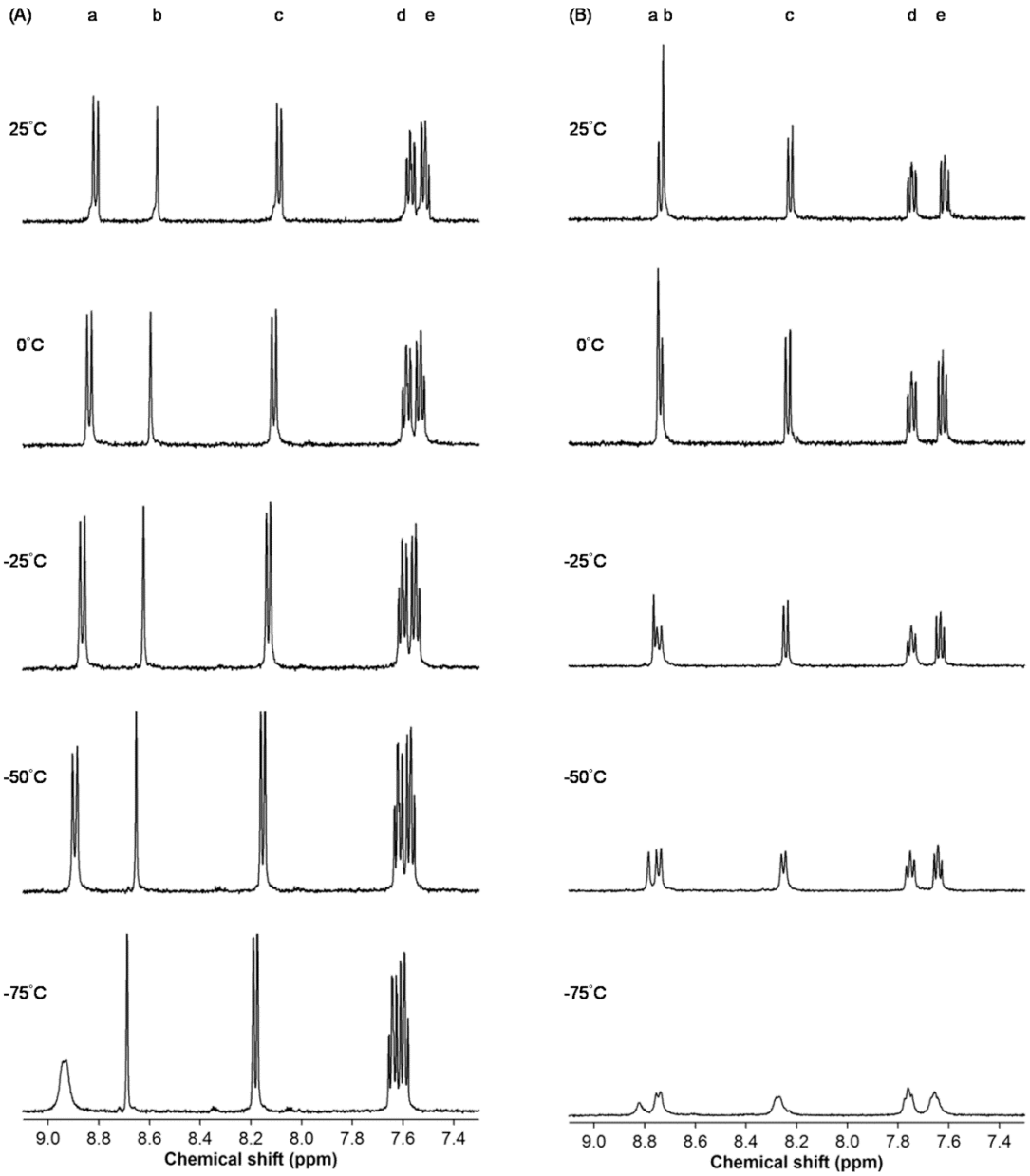

Fig. S3 Aromatic regions in the ^{1}H NMR spectra of **L1** (A) and **1** (B) in acetone-d_6 at varied temperatures from 25°C to −75°C. Signals a, b, c, d and e correspond to the protons at 1/8-, 10-, 4/5-, 2/7-, 3/6- positions of the anthracene moiety, respectively. The selective broadening of the signal a of **L1** is due to the slow rotation about the 9-anthryl-methylamine bond. See: W. B. Jennings, M. J. Kochanewycz, and L. Lunazzi, *J. Chem. Soc., Perkin Trans. 2*, **1997**, 2271-2273.

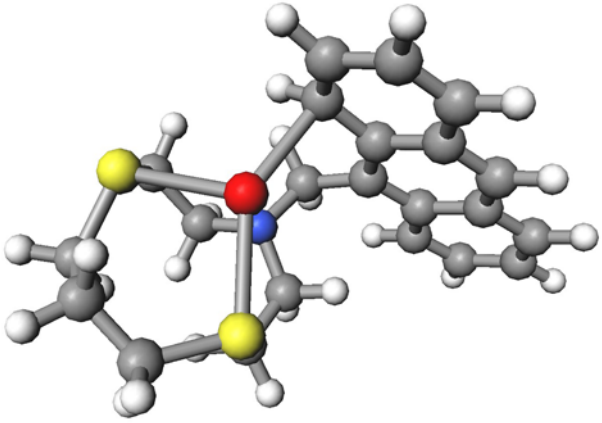

Fig. S4 Theoretically optimised structure of **1**.

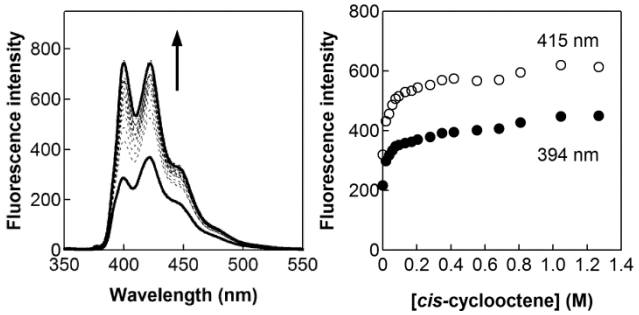

Fig. S5 Fluorescence spectral changes of **1** (64 μM) in chloroform on titration with *cis*-cyclooctene, measured with the excitation wavelength at 339 nm and slit widths at 2.5 nm. The arrows indicate spectral change with increasing the concentration of *cis*-cyclooctene. The inset shows changes in fluorescence emission at 394 nm (open circles) and 415 nm (closed circles) during the course of the titration.

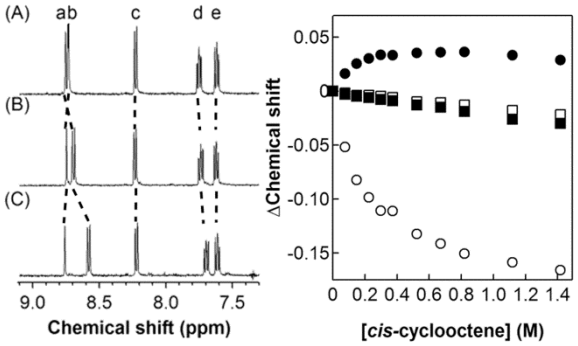

Fig. S6 ^{1}H NMR spectra of **1** (2.7 mM) and **L1** (2.7 mM) in acetone-d_6 at 25°C in the absence (A) and presence of 0.1 M (B) and 1.4 M (C) *cis*-cyclooctene at the range from 7.3 ppm to 9.1 ppm. Signals a, b, c, d and e correspond to the protons at 1/8-, 10-, 4/5-, 2/7-, 3/6- positions of the anthracene moiety, respectively. The right panel shows changes in the proton chemical shifts of signals a (○) and b (●) of **1** and signals a (□) and b (■) of **L1** in the presence of varied concentrations of *cis*-cyclooctene.

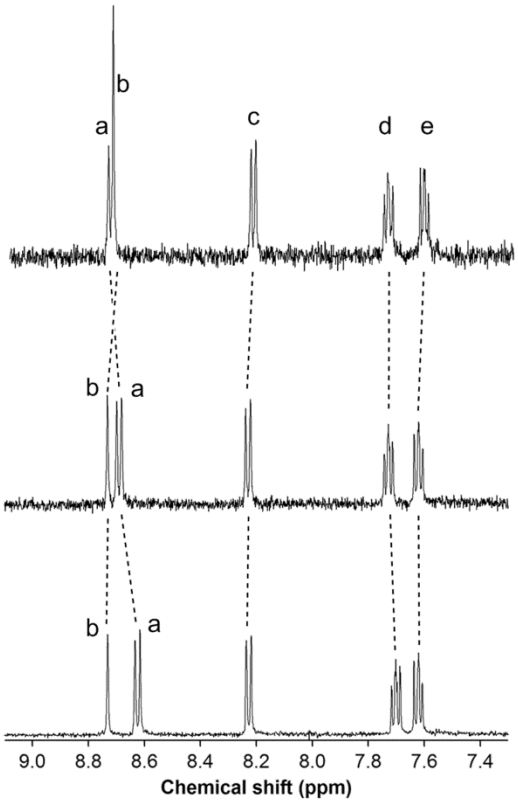

Fig. S7 ^{1}H NMR spectra of **1** in acetone-d_6 at 25°C in the absence (upper) and presence of 20 mM (middle) and 100 mM (lower) acetonitrile at the range from 7.3 ppm to 9.1 ppm.

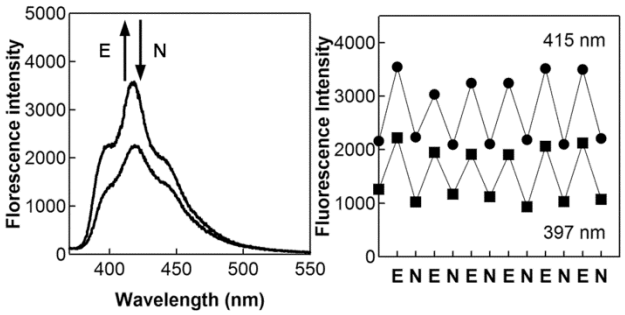

Fig. S8 Fluorescence spectra of **1** (0.58 mM) in chloroform at 25°C before (trace a, solid line) and after (trace b, dotted line) ethylene purge, measured with the excitation wavelength at 353 nm, excitation slit width at 1 nm and emission slit width at 10 nm. The right panel shows changes in fluorescence intensity at 394 nm and 415 nm during alternating purges of ethylene (E) and nitrogen (N).

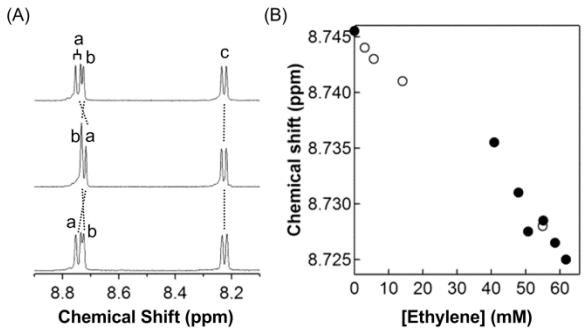

Fig. S9 ^{1}H NMR spectra of **1** (2.7 mM) in acetone-d_6 at 25°C from 8.1 ppm to 8.9 ppm. The initial solution (upper spectrum) was purged with ethylene gas (middle spectrum), and then, with nitrogen gas (lower spectrum) (A). The right panel shows chemical shifts of the proton at the 1/8 positions of the anthracene moiety against the concentration of ethylene in the solution (B). The data were taken by first gradually increasing the ethylene concentration (filled circles), and then, decreasing it by purging with nitrogen (open circles).

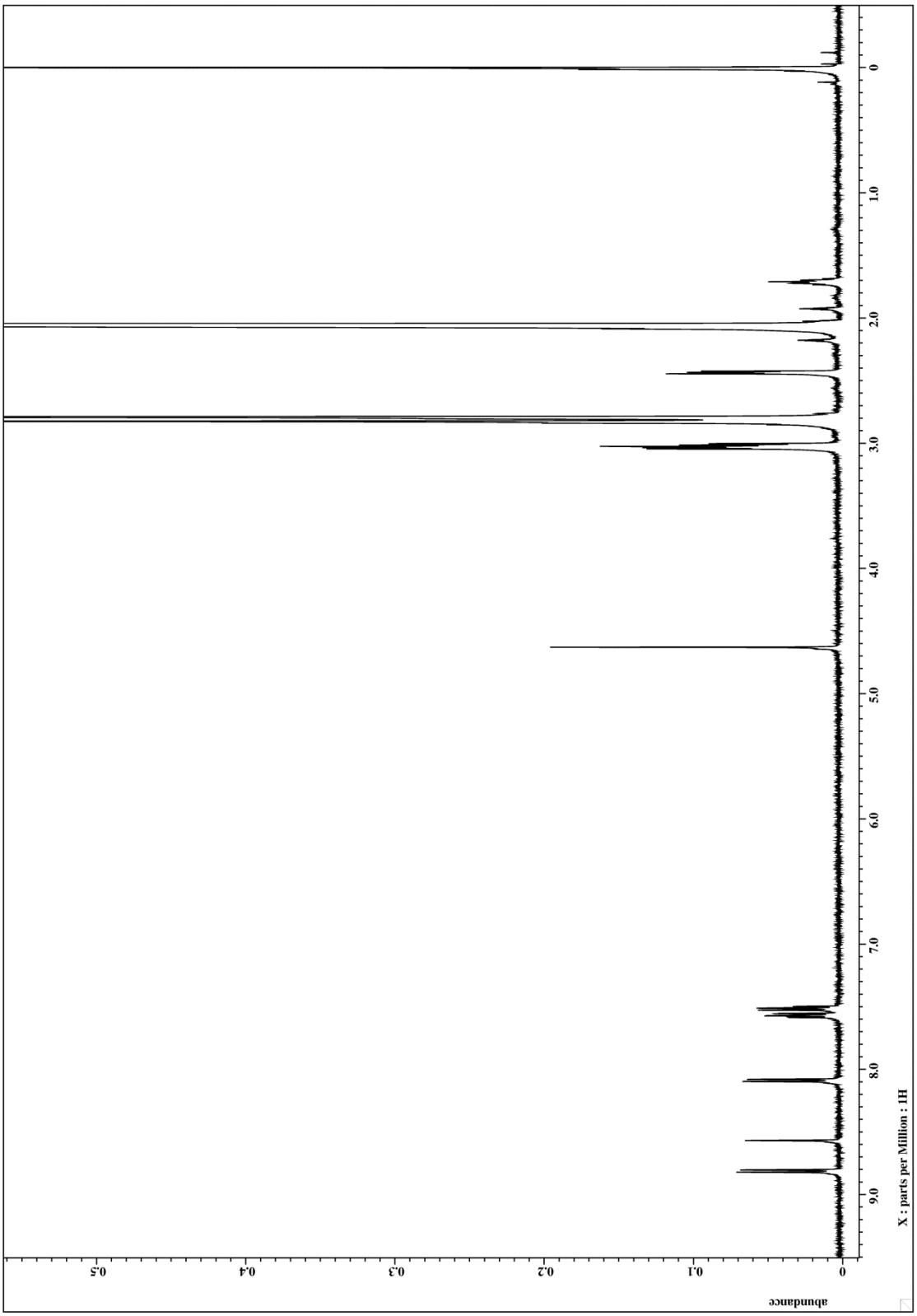

Fig. S10 ^{1}H NMR spectrum of **L1** in acetone-d_6 at 25°C.

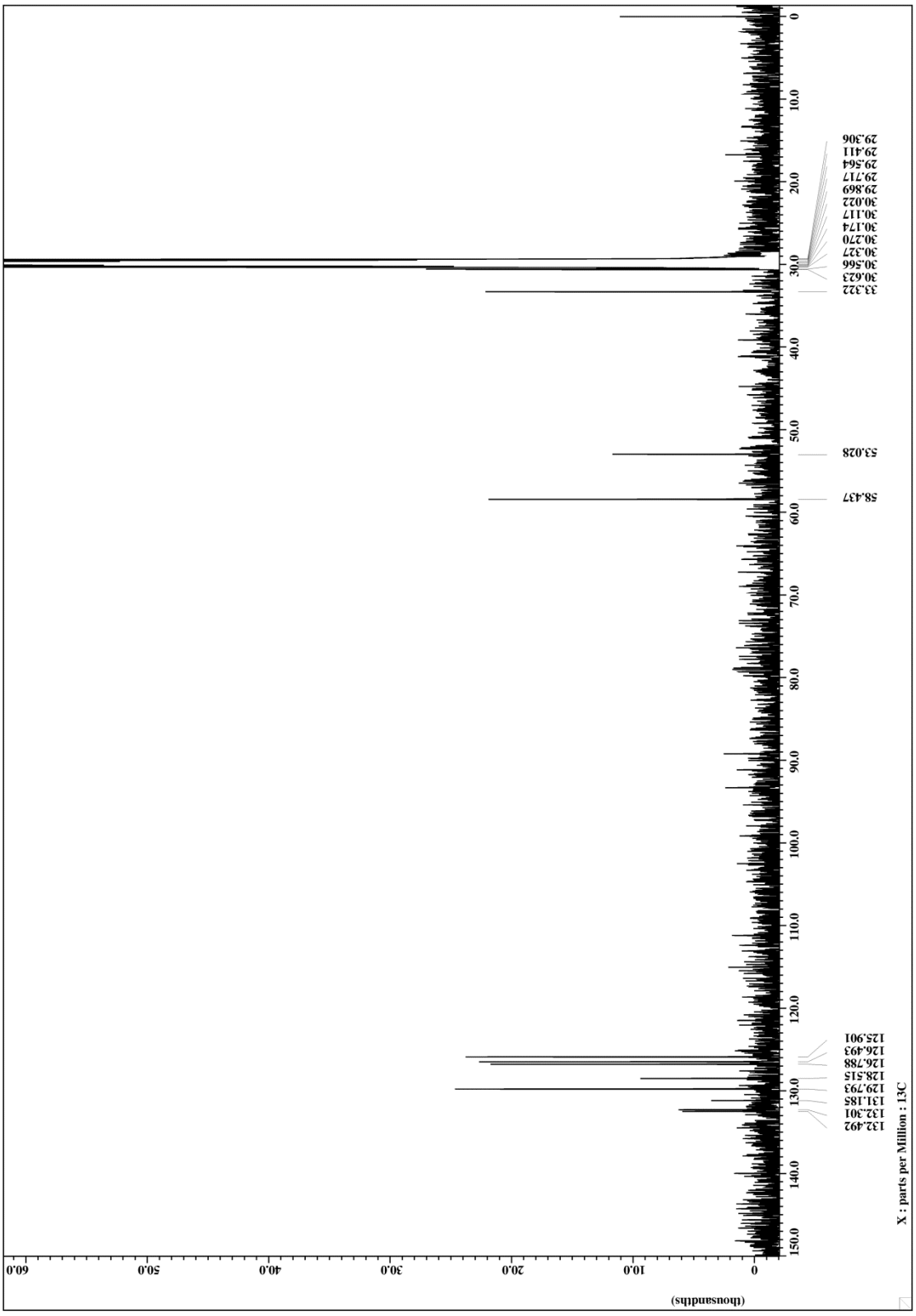

Fig. S11 ^{13}C NMR spectrum of **L1** in acetone-d_6 at 25°C.

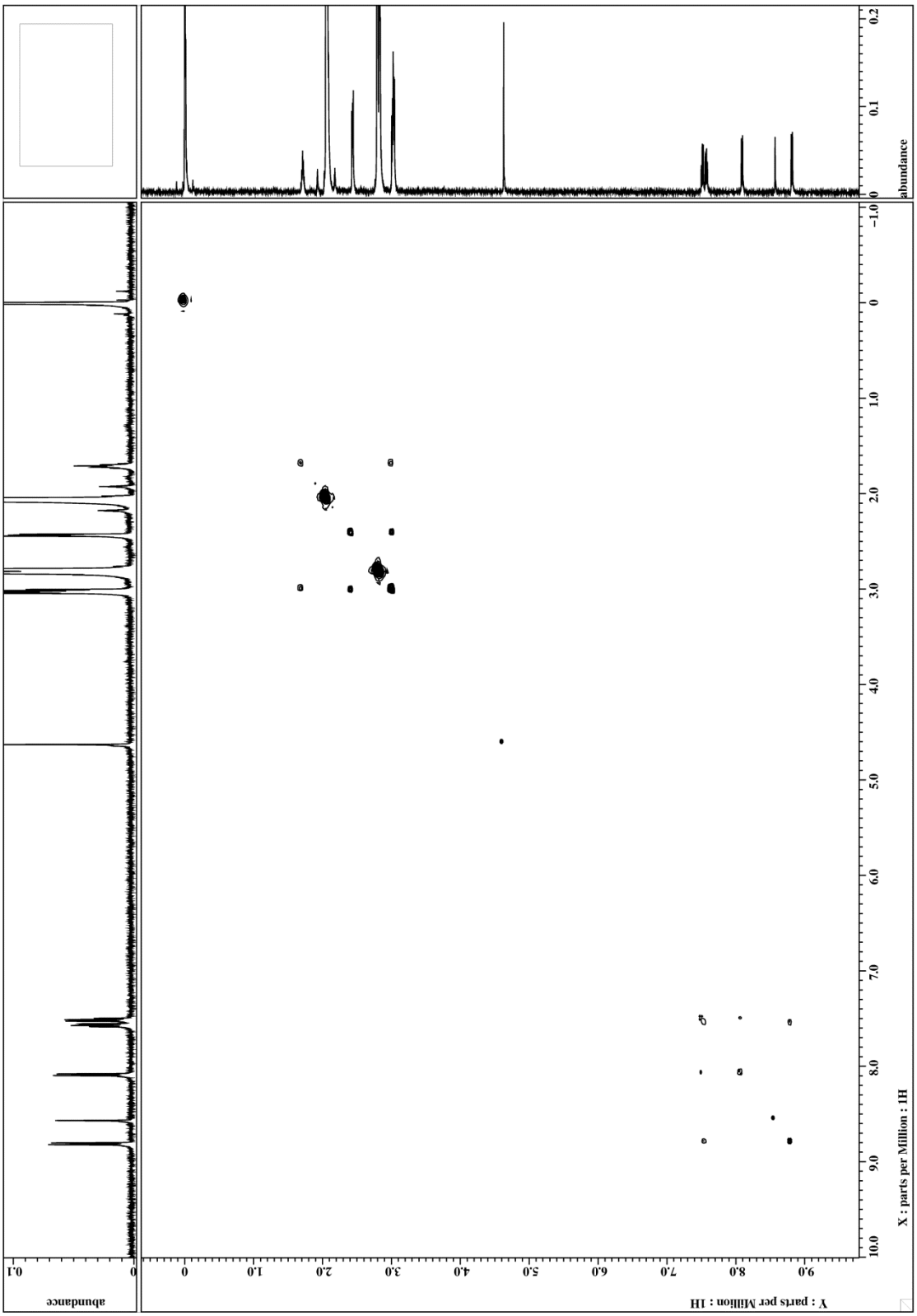

Fig. S12 ^{1}H-^{1}H COSY spectrum of **L1** in acetone-d_6 at 25°C.

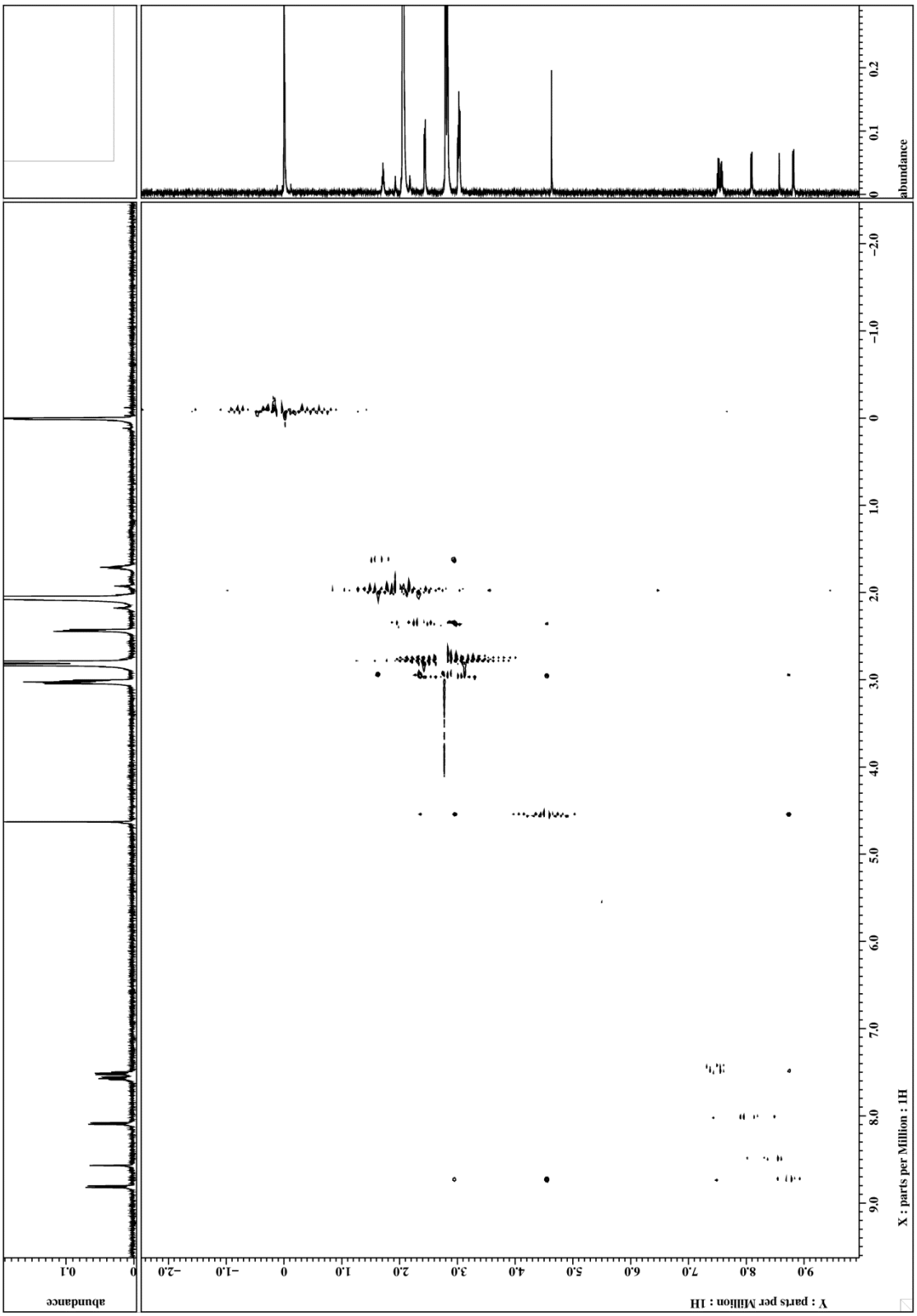

Fig. S13 NOESY spectrum of **L1** in acetone-d_6 at 25°C.

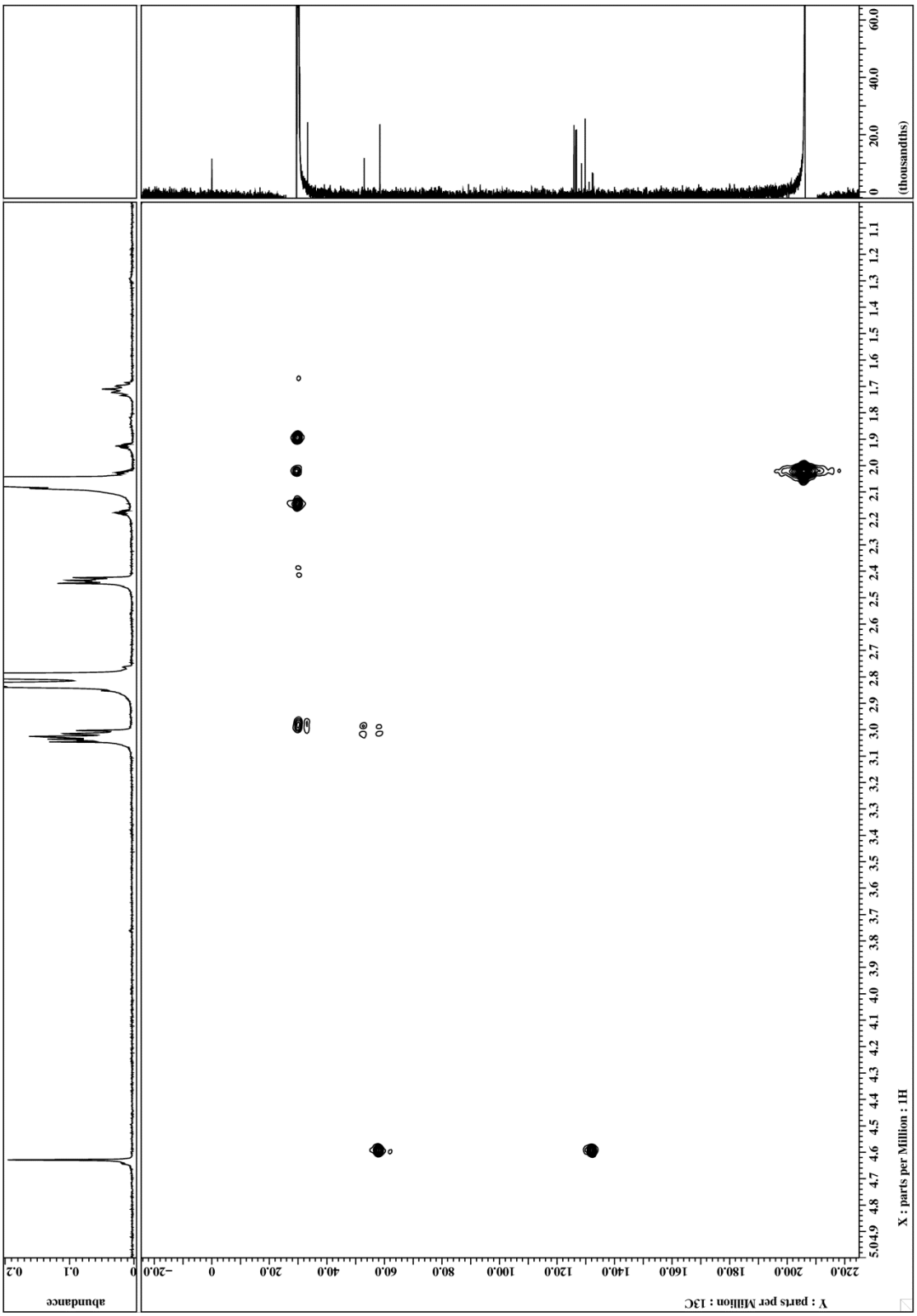

Fig. S14 HMBC spectrum of **L1** in acetone-d_6 at 25°C (aliphatic region).

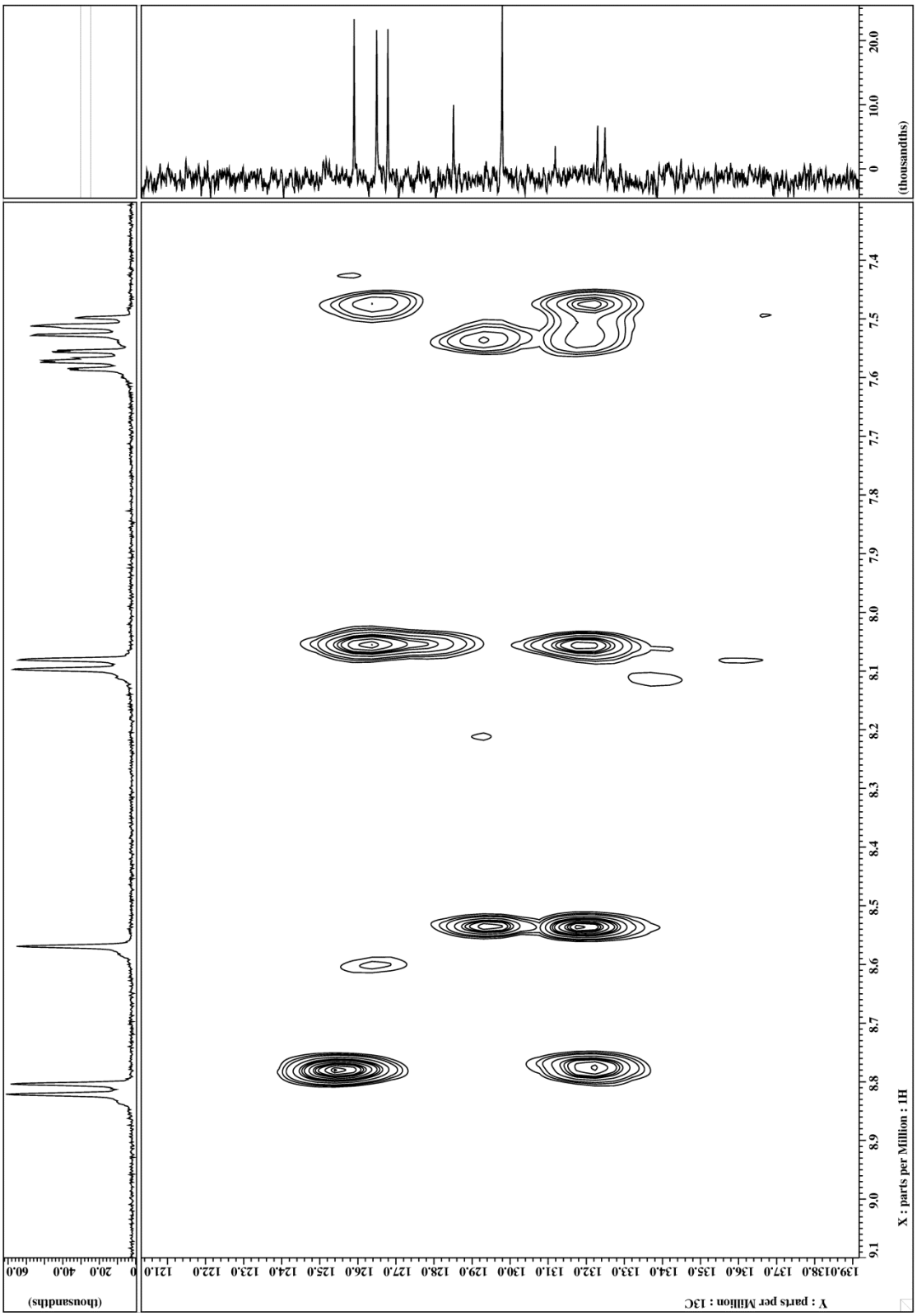

Fig. S15 HMBC spectrum of **L1** in acetone-d_6 at 25°C (aromatic region).

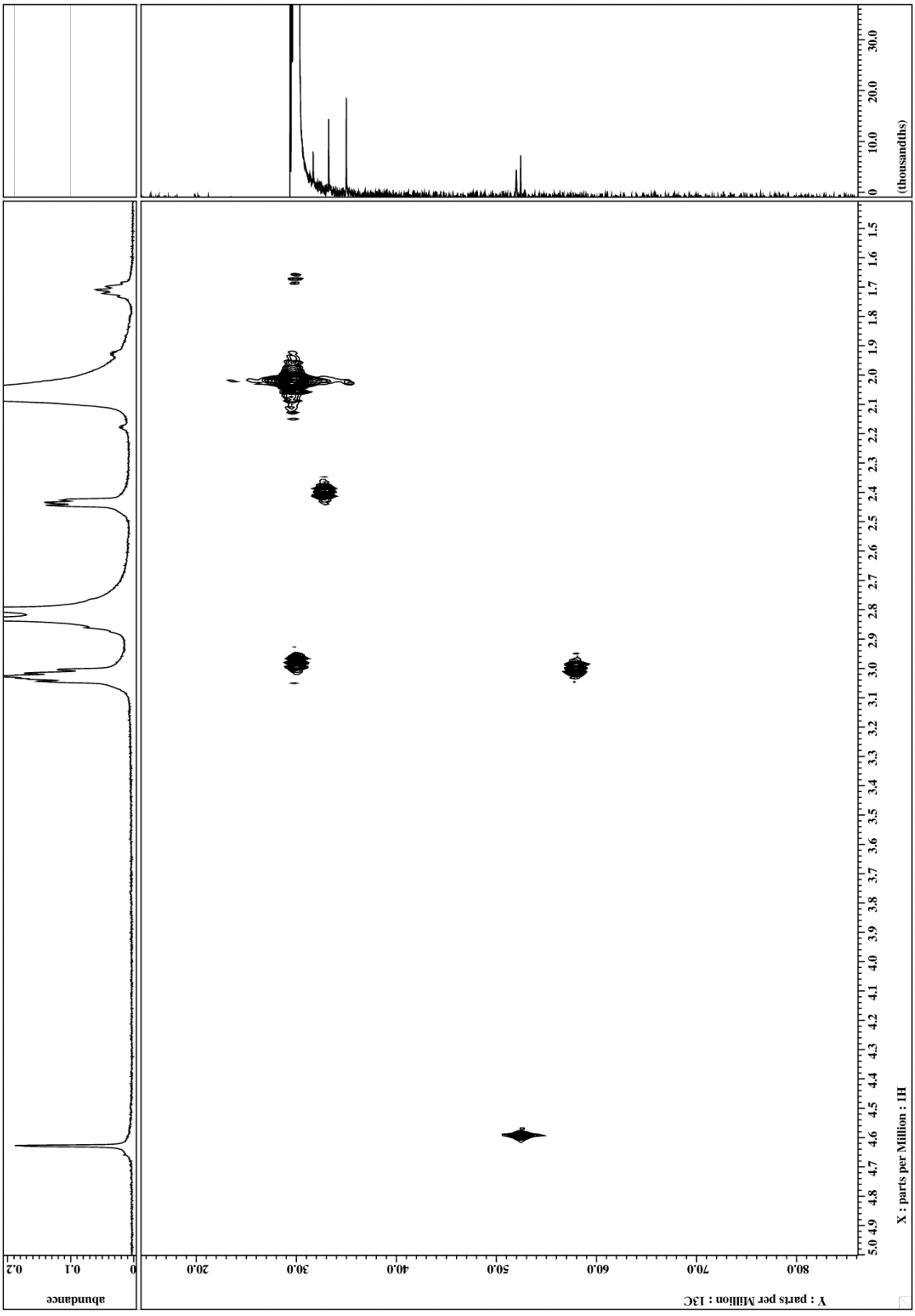

Fig. S16 HMQC spectrum of **L1** in acetone-d_6 at 25°C (aliphatic region).

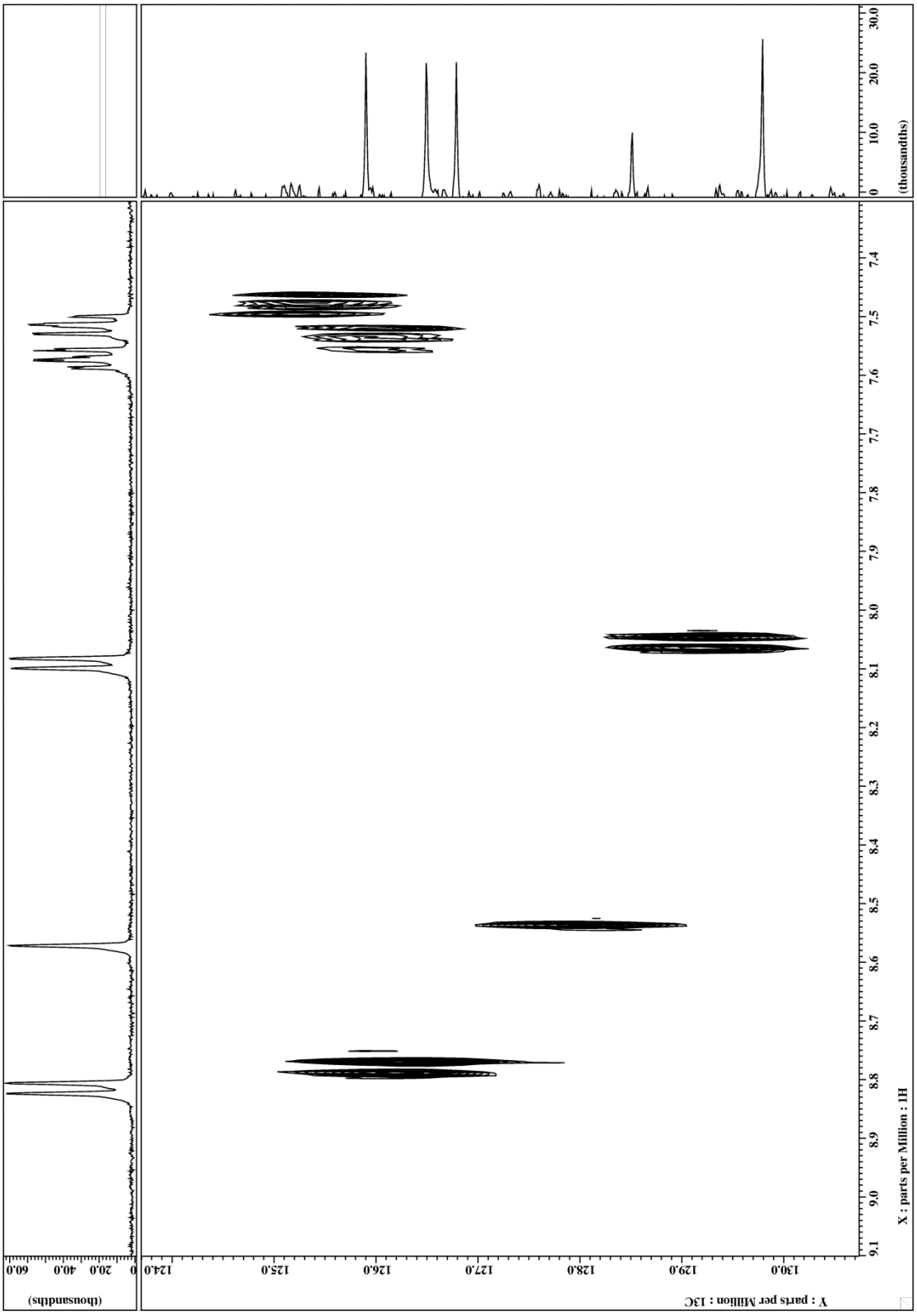

Fig. S17 HMQC spectrum of **L1** in acetone-d_6 at 25°C (aromatic region).

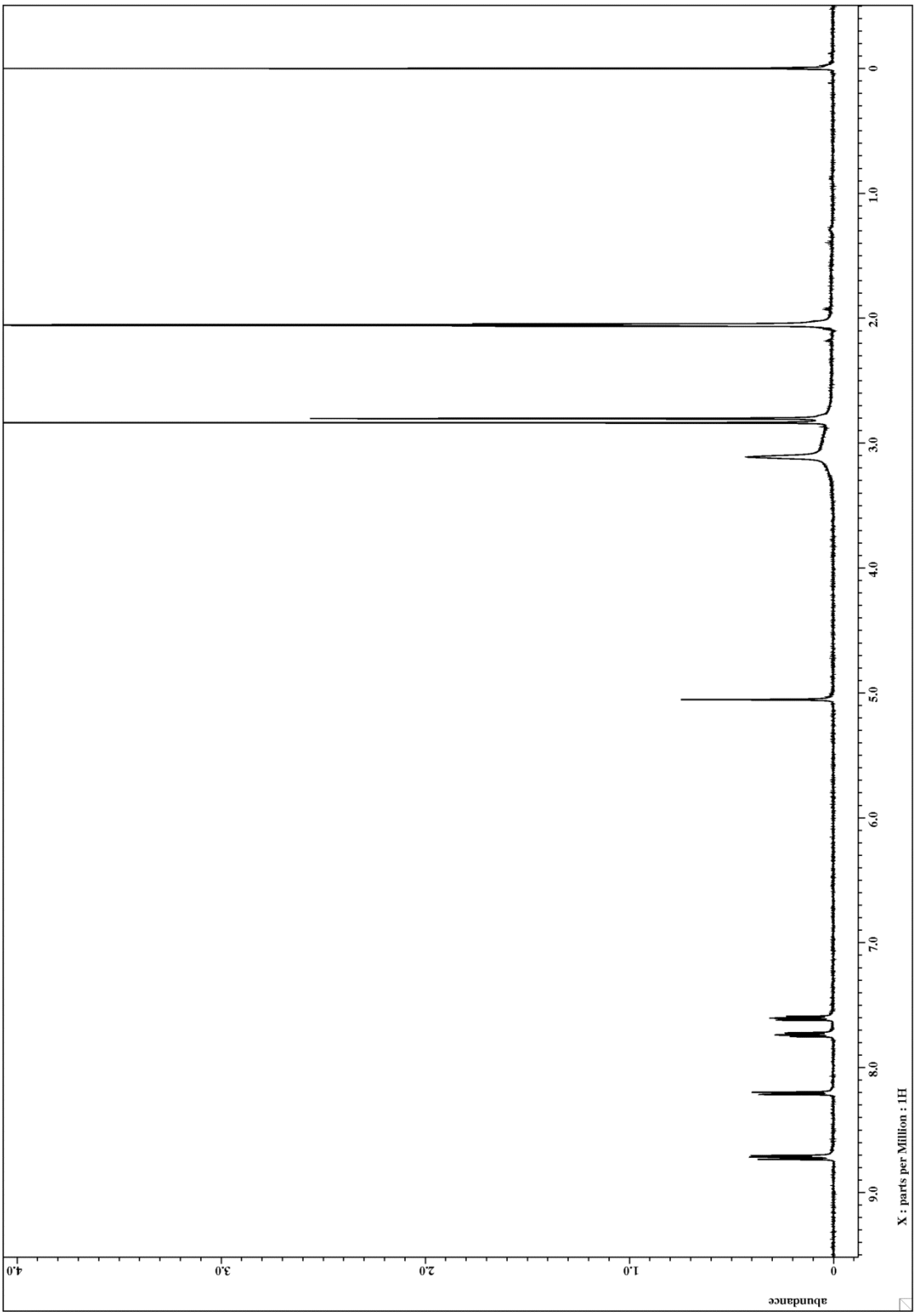

Fig. S18 ^{1}H NMR spectrum of **1** in acetone-d_6 at 25°C.

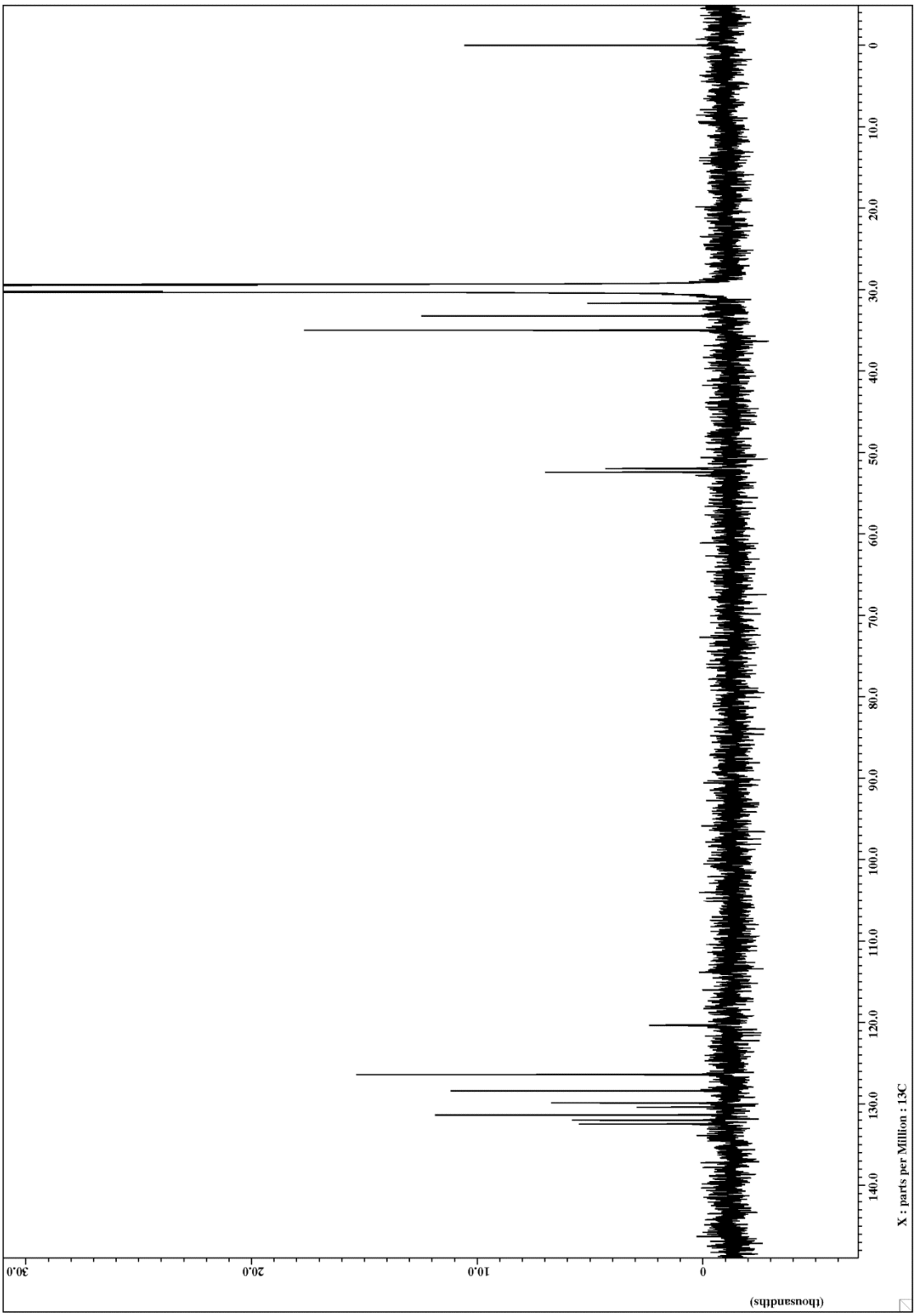

Fig. S19 ^{13}C NMR spectrum of **1** in acetone-d_6 at 25°C.

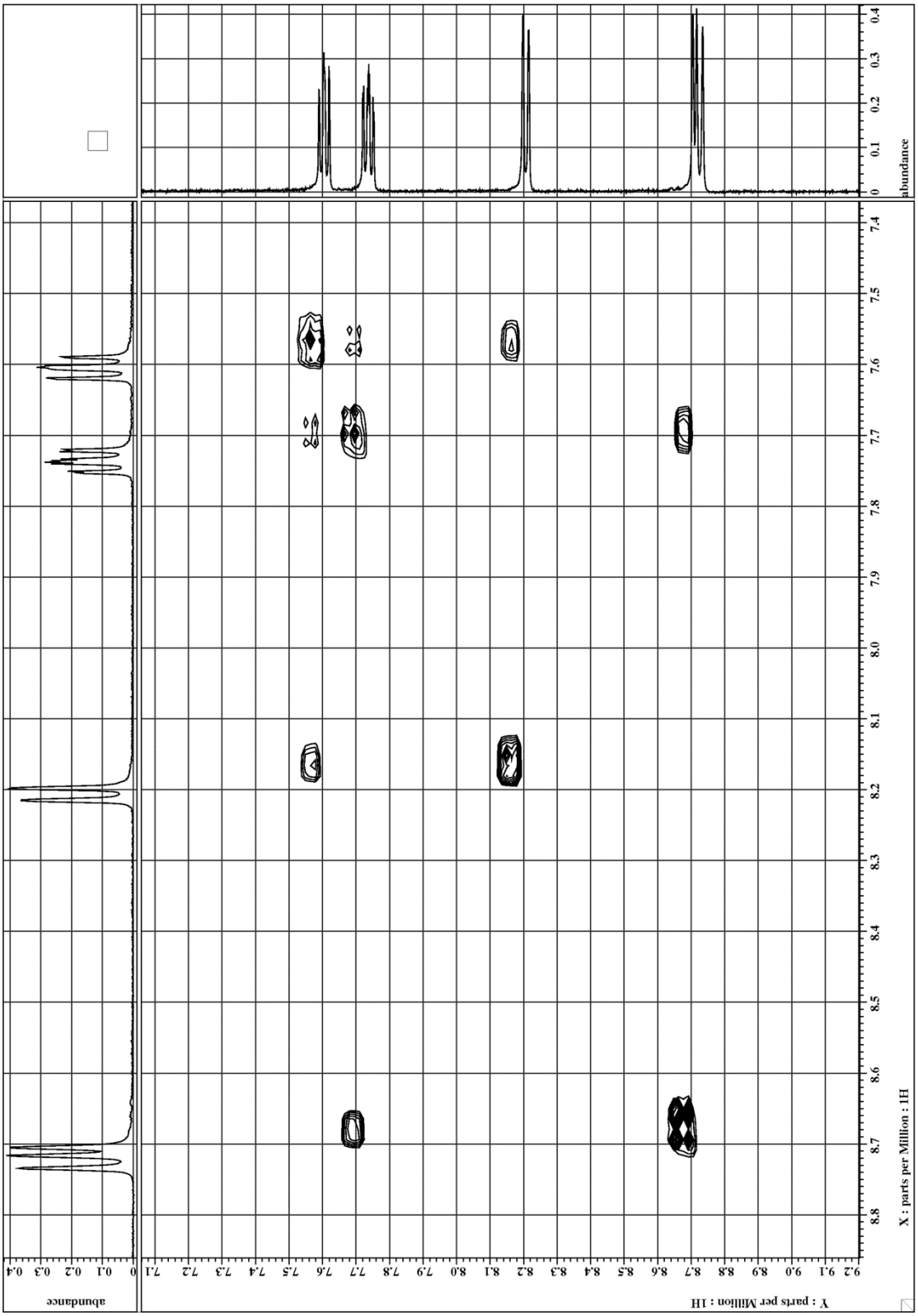

Fig. S20 ^{1}H-^{1}H COSY spectrum of **1** in acetone-d_6 at 25°C.

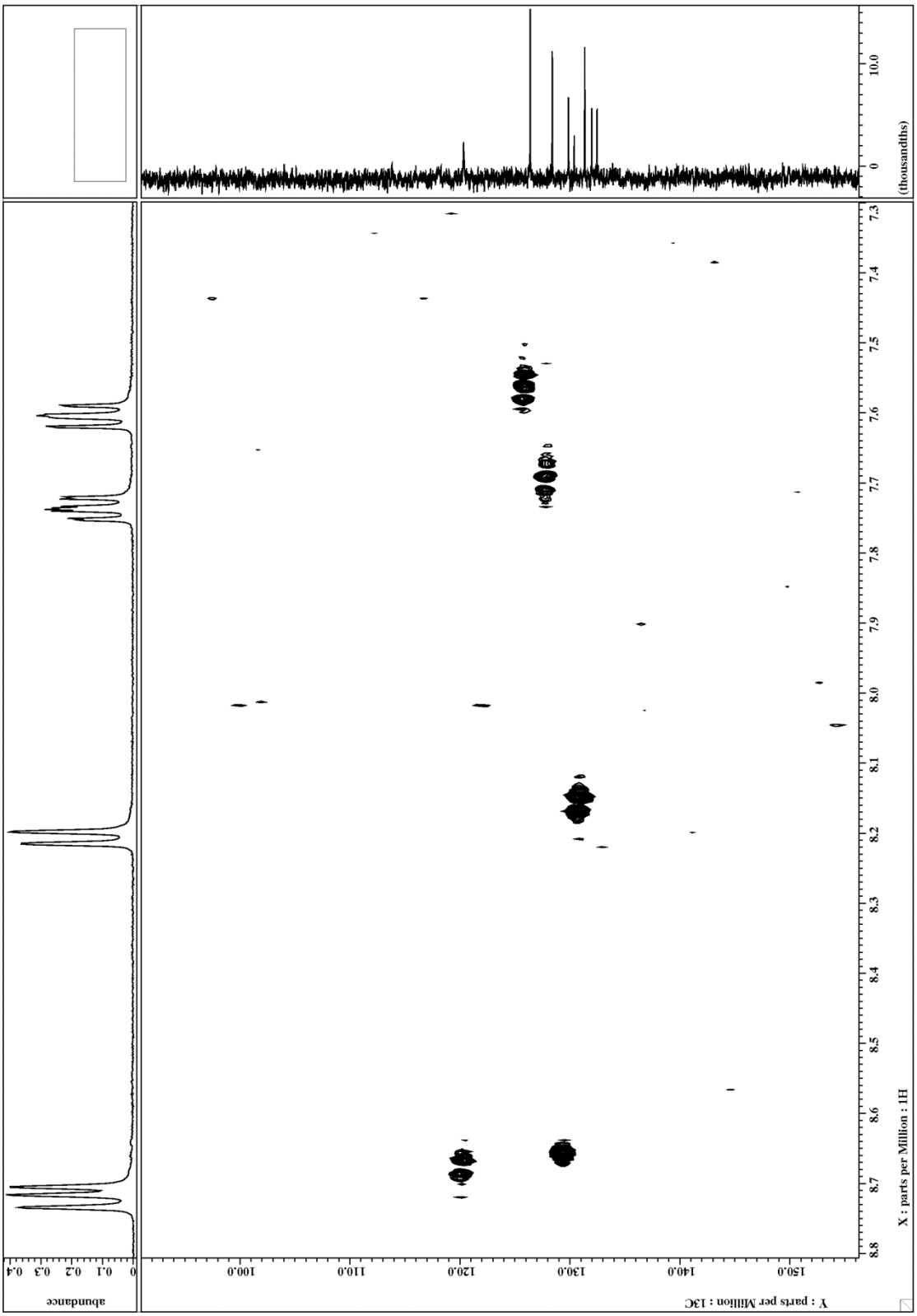

Fig. S21 HMQC spectrum of **1** in acetone-d_6 at 25°C (aromatic region).

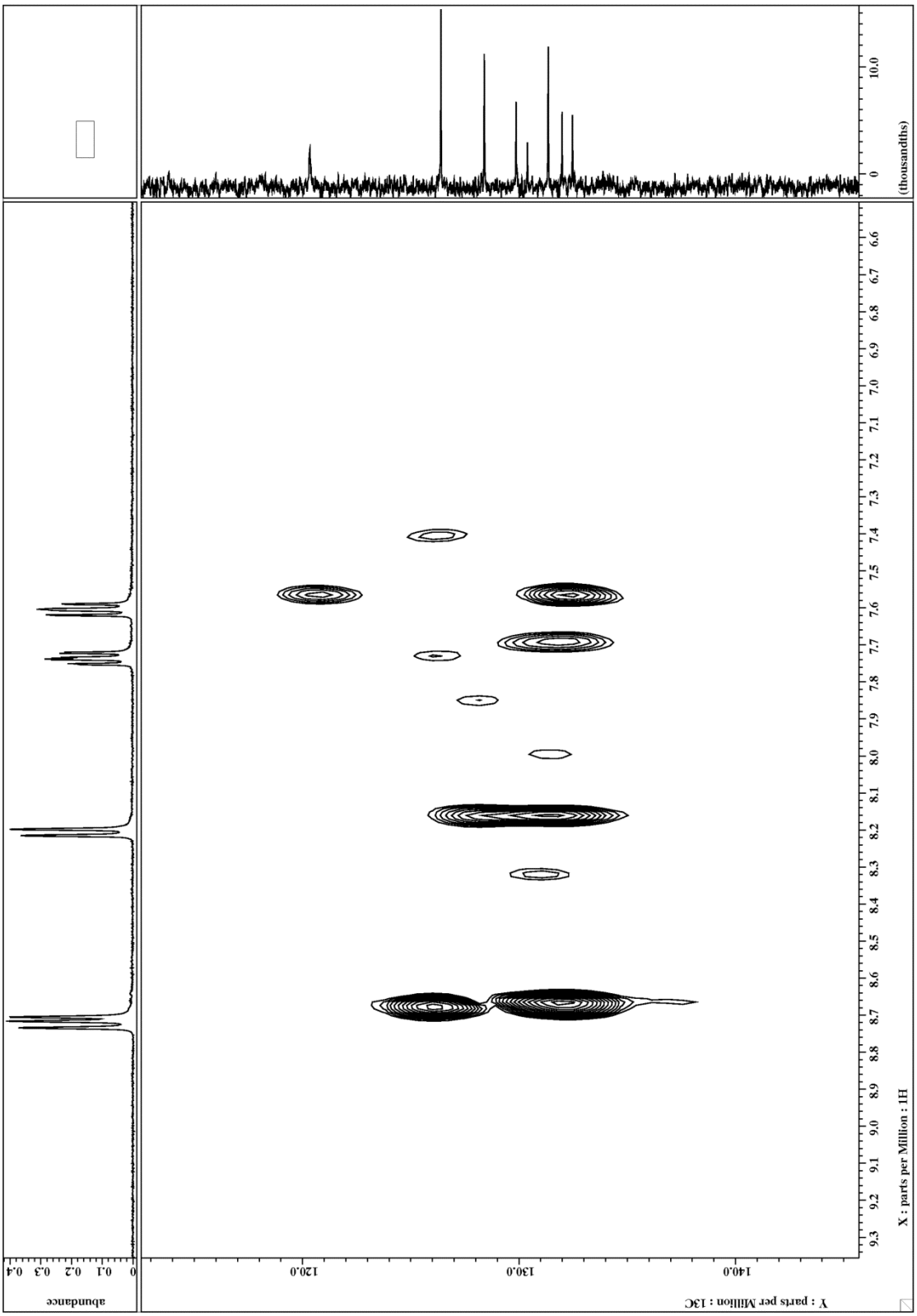

Fig. S22 HMBC spectrum of **1** in acetone-d_6 at 25°C (aromatic region).

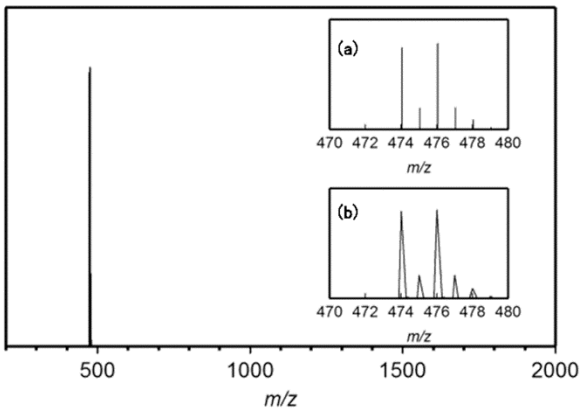

Fig. S23 Electrospray ionisation mass spectrum of **1** (positive mode). Needle voltage: 2000 V, ring lens voltage: 10 V, olifice1: 20 V, olifice2: 25 V, solvent: MeOH, flow: 0.120 mL sec^{-1}. The insets show the simulated isotope pattern of $[Ag(\mathbf{L1})]^+$ (a), together with the observed one (b).

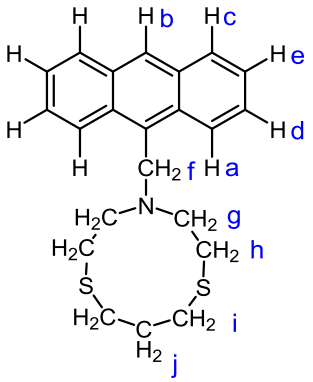

a: 8.82 (d, J = 8.9 Hz, 2H)
b: 8.57 (s, 1H)
c: 8.09 (d, J = 8.1 Hz, 1H)
d: 7.57(dd, J = 8.9, 6.7 Hz, 2H)
e: 7.51 (dd, J = 8.1, 6.7 Hz, 2H)
f: 4.63 (s, An-CH_2-N, 2H)
g and **i**: 3.05-3.01 (m, 8H)
h: 2.45-2.43 (m, 4H)
j: 1.73-1.68 (m, 2H)

Fig. S24 Assignment of ^{1}H chemical shifts of **L1** in acetone-d_6.

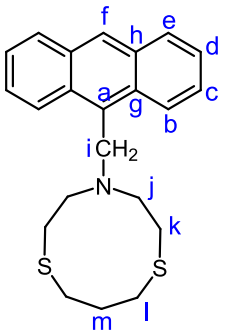

a: 131.2
b: 126.8
c: 126.5
d: 125.9
e: 129.8
f: 128.5
g: 132.5
h: 132.3
i: 53.03
j: 58.4
k: 33.3
l: 30.6
m: 30.6

Fig. S25 Assignment of ^{13}C chemical shifts of **L1** in acetone-d_6.

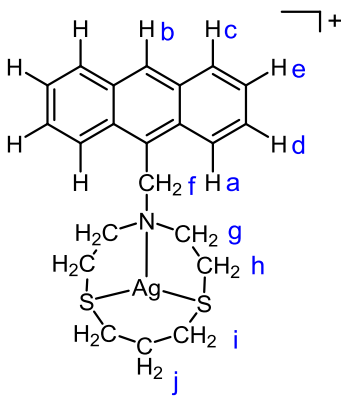

a: 8.73 (d, *J* = 9.1 Hz, 2H)
b: 8.71 (s, 1H)
c: 8.21 (d, *J* = 8.6 Hz, 1H)
d: 7.74 (dd, *J* = 9.1, 6.2 Hz, 2H)
e: 7.60(dd, *J* = 8.6, 6.2 Hz, 2H)
f: 5.05 (s, 2H)
g to **j**: 3.11-1.35 (br, 14H)

Fig. S26 Assignment of ^{1}H chemical shifts of **1** in acetone-d_6.

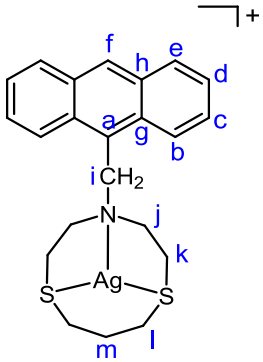

a: 130.4
b: 120.3
c: 128.4
d: 126.4
e: 131.4
f: 129.9
g: 132.0
h: 132.5
i: 52.4
j: 52.0
k: 35.0
l: 33.2
m: 31.7

Fig. S27 Assignment of ^{13}C chemical shifts of **1** in acetone-d_6..

Table S1. Cartesian coordinate of the optimised structure of **1** (Å).

element	x	y	z
Ag	1.087287	-2.12418	1.323327
S	-1.16609	-3.10987	2.137293
S	1.627115	-0.47652	3.320208
C	-1.06763	-3.09954	3.995841
H	-1.10595	-4.16644	4.254828
H	-2.01135	-2.65554	4.343667
C	0.143306	-2.45956	4.680022
H	1.06533	-2.97143	4.361791
H	0.037691	-2.69502	5.752397
C	0.307746	-0.93239	4.545539
H	0.613516	-0.49062	5.501407
H	-0.62951	-0.44888	4.241949
C	0.964989	1.031294	2.48156
H	1.780409	1.312997	1.79937

H	0.885546	1.834748	3.227167
C	-2.20541	-1.6026	1.776223
H	-2.24994	-1.01627	2.701944
H	-3.22001	-1.9695	1.572575
C	-1.75357	-0.76558	0.57761
H	-2.53552	0.005998	0.416005
H	-1.7478	-1.39397	-0.32325
N	-0.41416	-0.15347	0.69865
C	-0.37202	0.886314	1.74627
H	-1.15762	0.674399	2.483479
H	-0.62428	1.8787	1.321242
C	0.062733	0.399494	-0.61438
H	1.03897	0.868811	-0.42296
H	-0.60518	1.216715	-0.9328
H	-3.47839	0.823224	-4.14268
C	-2.69852	0.073045	-4.00467
H	-1.90955	1.063808	-2.30416
C	-1.8102	0.202118	-2.96255
C	-1.62204	-1.95474	-4.75123
C	-0.75749	-0.74473	-2.75249
C	-2.60965	-1.01663	-4.91207
C	-0.67622	-1.85485	-3.68543
C	0.189699	-0.65302	-1.69554
H	-3.32279	-1.09866	-5.73268
H	0.335889	-3.68694	-4.19515
H	-1.53667	-2.79686	-5.44044
C	1.238443	-1.60212	-1.60602
C	2.313933	-1.49575	-0.64905
C	1.271329	-2.7372	-2.50297
H	2.273225	-4.58853	-3.02592
C	0.311733	-2.83133	-3.51625
C	3.270769	-2.49593	-0.52455
H	2.487176	-0.54319	-0.14283
H	4.107261	-2.35612	0.162412
C	3.2312	-3.64807	-1.35648
H	3.988544	-4.42361	-1.24306
C	2.277784	-3.73899	-2.34026